Telocytes are a critical source of Wnts essential for hair follicle regeneration

Marco Canella [1] , Simcha Nalick [1] , Noa Corem [1] , Amal Gharbi [1] , Ittai Ben-Porath [1] and Michal Shoshkes-Carmel [1]

[1]Department of Developmental Biology and Cancer Research, Institute for Medical Research Israel-Canada, Hebrew University Medical School, Jerusalem, Israel;

Corresponding author: Michal Shoshkes-Carmel
Institute for Medical Research Israel-Canada
Hebrew University Medical School, Jerusalem, Israel
phone: +972-2-6758511, fax: +972-2-6757482
email: Michal.shoshkes@mail.huji.ac.il

ABSTRACT

In multiple tissues, stem cell proliferation driving tissue regeneration is dependent on Wnt/β-catenin signaling, but the identity of the niche cells providing the Wnt proteins is not resolved. Here, we show that telocytes, unique interstitial cells that harbor long cytoplasmic extensions, are obligatory Wnt-producing niche cells in the hair follicle. Employing two independent mouse models we reveal a continuous network of interconnected telocytes that envelopes stem cells and their progeny along the path of differentiation. Telocytes compartmentalize in space and time the production of mRNA molecules that encode important signaling factors, for localized phase-dependent signaling. Ablation of either dermal telocytes, or the Wnt signals emanating from them, abrogates hair follicle regeneration, demonstrating that telocytes constitute a critical component of the hair follicle stem cell niche. We propose that telocyte production of Wnt is a universal theme in adult stem cell biology and tissue regeneration.

Self-renewing tissues, such as the intestine and skin, rely on stem cells as the engine to fuel regeneration and replenish differentiated cells. Stem cell function is supported by specialized niches in different tissue domains determined by local cues[1-3]. In the intestine, epithelial cells are spatially organized along repetitive crypt-villus axes, in which rapidly cycling stem cells expressing Lgr5 reside at the crypt base[4]. The skin epithelium consists of the keratinized epidermis which protects the organism from the environment, and prominent structures derivatives of the epidermis which extend into the dermis, such as the sweat glands, sebaceous glands and hair follicles. In mice, much of the skin is covered by a hair coat that regenerates in sequential cycles of growth (anagen), regression (catagen) and resting (telogen) phases. During the anagen phase, Lgr5 and K15/CD34 expressing stem cells located at the bulge, the bottom part of the permanent hair follicle proliferate to form progenitors called matrix cells. Matrix cell proliferation produces the inner root sheath, which remains in close contact with a mesenchymal component, the dermal papilla. In turn, cells extensively disperse downwards and along radial axes generating concentric layers of cells which undergo terminal differentiation along the hair shaft[2,5,6].

Regulation of hair follicle homeostasis is carefully controlled via a tight balance between cell proliferation and terminal differentiation. Wnt/β-catenin signaling is the driving force for hair follicle development and growth[7-18]. Though the need for active Wnt-signaling in the stem cell compartment is well established, the cellular composition of the stem cell niche, which provides Wnt proteins essential to induce proliferation, is still a matter of debate. An autocrine mechanism in which stem cells themselves produce Wnt signals has been suggested to control hair follicle and interfollicular epidermis stem cell proliferation[19,20]. Likewise, it has been proposed that basal placode progenitor cells play an important role in controlling their own stem cell identity by serving as a source of Wnts and Wnt activators[21] and by signaling to the dermal fibroblasts[22]. Ouspenskaia *et al*. proposed a mechanism by which stem cell specification and regulation are niche-independent but result from asymmetric cell divisions that differentially display Wnt and Shh signaling, respectively[23].

Mesenchyme-epithelium cross-talk has long been thought to play an important role in hair follicle morphogenesis and regeneration. The position of the

dermal papilla, a specialized mesenchymal component, in close proximity to the bulge and proliferating progenitors drew much attention as a potential mesenchymal signaling hub that could induce regeneration. Starting from the early 60s, comprehensive studies using mainly grafting, transplantation, and laser ablation assays, have highlighted the instructive role of the dermal papilla in hair growth even in non-appendageal sites[2,24-28]. Work from the Watt lab revealed that dermal papilla are polyclonal and contain mitotically inactive cells[24], whereas transcriptional profiling of the dermal papilla, isolated by multicolor labeling approach, and of the hair follicle mesenchyme, revealed that the dermal papilla express potential niche supporting pathways which distinguish them from other mesenchymal cells[6,25,26]. In addition to the dermal papilla, a much less studied mesenchymal component is the dermal sheath that lines the hair follicle. Dermal sheath cells express alpha smooth muscle actin (αSMA) and were shown to contract during the resting phase in order to relocate the dermal papilla to the stem cell reservoir following hair follicle regression[29-32]. Both the dermal sheath and the dermal papilla are thought to be derived from the same embryonic component, the dermal condensate[28]. Similar to the dermal papilla, dermal sheath transplantation assays have also been shown to induce *de novo* hair follicle formation[33,34]; however, the heterogeneity within the dermal sheath or the dermal papilla compartments and their potential role as a source for Wnt ligands playing a role in hair follicle regeneration remains elusive.

Recently, a specialized mesenchymal cell type termed telocyte was identified as a critical niche component in the intestinal crypt. These cells express the transcription factor Forkhead Box l1 (Foxl1) and form a subepithelial network that is crucial for intestinal homeostatic regeneration, serving as essential source of Wnt ligands[35,36]. Given their role in the intestine, we hypothesized that a telocyte network may also be operative in the hair follicle. In the skin, telocytes were previously only characterized by EM, based on their unique cellular structure, or by immunofluorescence labeling for CD34 or CD34/PDGFRα. Telocytes were reported to form a network around hair follicles in the bulge and sub-bulge regions and were proposed to take part in skin regeneration; however, such a role was not investigated experimentally[37-41]. Although telocytes were described in the adult skin and hair follicle mesenchyme, Foxl1 expression has only been reported during skin

development in the dermal condensate compartment lying underneath the developing hair follicle placode[42].

Here, we revealed a comprehensive 3D network of inter- and sub-follicular telocytes along all hair follicle epithelial cell layers in close apposition to stem, progenitor and differentiated cells. Remarkably, telocytes compartmentalize mRNA molecules encoding important signaling factors spatiotemporally for localized phase-dependent signaling. Using two independent mouse models to specifically ablate dermal telocytes themselves or Wnt signals emanating from them we show that Foxl1 telocytes are a critical source of Wnt proteins essential for hair follicle regeneration and thus constitute the hair follicle stem cell niche.

RESULTS

Foxl1 labels a network of mesenchymal cells with long cellular extensions which integrates with hair follicle epithelial layers.

In order to examine whether Foxl1 is expressed and can be used as a marker to label telocytes in the skin, we employed Foxl1-promoter-driven Cre in conjunction with Rosa-mTmG reporter mice, encoding a plasma membrane-bound version of green fluorescence protein (GFP), which allows visualization of the structure of Foxl1-expressing cells[35] (**Fig. 1a** diagram). Given the physical characteristics of telocytes, harboring thin membranous cellular extensions, we performed whole animal trans-cardiac perfusion with 4%PFA to better preserve cellular structures (for details see methods) and dissected the mouse back skin. To appreciate the full extent of the 3D network of Foxl1+ cells we performed spinning disk imaging of immunofluorescent stained whole adult mouse skin following tissue clearing. 3D image reconstruction exposed an extensive network of Foxl1/GFP cells tightly associated with hair follicles. The GFP+ array was composed of inter-follicular elongated cells with small cell bodies and very long processes, reaching hundreds of microns in length, spanning multiple hair follicles (**Fig. 1b**). Next, we followed the distribution of Foxl1/GFP cells during the growth phase of hair follicle regeneration to explore the relationship between Foxl1/GFP cells and hair follicle stem cell activity. Hair follicle morphogenesis in mice ends on p21 and is followed by a second anagen phase beginning on p24, in which hair growth is synchronized. We used reporter mice on p30-33, a stage at which hair follicle growth is at the peak of the anagen

phase. In full anagen, we observed a thin GFP-labeled sheath of cells encapsulating the entire hair follicle. The Foxl1/GFP sub-follicular network was attached to the basal side of the outer epithelial layer with cell processes oriented towards the follicles as visualized by P-cadherin (P-Cad) staining (**Fig. 1c,d**). Notably, in skin dissected from p30-33 mice which were fixed in 4%PFA at 4°C overnight without perfusion, the GFP+ cellular structure was not detected (**Extended Data Fig. 1a,b**), highlighting the importance of proper fixation conditions in order to visualize Foxl1/GFP network.

Longitudinal and cross-sectioning throughout the hair follicle structure to follow the Foxl1/GFP network along the inner epithelial layers revealed a comprehensive sub-epithelial network of cells along all concentric cell layers. The outer root sheath, inner root sheath and hair shaft telocytes exist in or continuum with known mesenchymal components, such as the dermal sheath (**Fig. 1f** arrowhead), dermal sheath cup which surrounds the dermal papilla (**Fig. 1g** arrow) and the dermal papilla (**Fig. 1f,g** asterisk). The expression of Foxl1 in GFP-labeled cells was confirmed by single molecule-fluorescence *in situ* hybridization (smFISH) (**Fig. 1e**). To better characterize the relationship of Foxl1/GFP to inner epithelial layers, we examined cross sections in the upper hair shaft or bulge regions, and co-stained for keratin 14 (K14) to label differentiated keratinocytes or keratin 15 (K15) to label stem cells. Foxl1-expressing GFP+ cellular extensions wrapped around the inner epithelial layers in intimate contact with both K14-expressing differentiated cells (**Fig. 1h**) and with K15-expressing stem cells (**Fig. 1i**, **Video 1**). To validate and extend our findings, we next used an inducible Foxl1;CreERT2 mouse model[43] crossed with the Rosa-mTmG reporter line (**Fig. 1j** diagram) and induced GFP expression at the onset of anagen using tamoxifen. This model enabled us to better visualize Foxl1+ cell bodies. As shown in Fig. 1k,l, GFP+ cell bodies were intercalated among K15+ stem cells at the bulge region.

Thus, Foxl1 is expressed in cells with long cellular processes which form a continuous subepithelial network which integrates with all hair follicle concentric cell layers in the outer root sheath, inner root sheath and hair shaft. Based on these properties we termed these cells telocytes.

Foxl1+ telocytes compartmentalize mRNA molecules of signaling proteins for localized, phase-dependent signaling

In order to gain a better understanding of the identity of telocytes in relation to previously described mesenchymal components, we stained skins of Foxl1Cre; Rosa-mTmG mice at anagen. The outside of the growing hair follicle is covered by an αSMA/PDGFRα-expressing dermal sheath[30]. It can clearly be seen that the peripheral telocytes (green) wrapped around the outermost layer of the hair follicle were co-labeled with αSMA or PDGFRα (red) (**Fig. 2a,c** arrowhead), suggesting that the peripheral telocytes belong to the dermal sheath component, whereas GFP+ cells located at the dermal papilla were αSMA or CD34 negative (**Fig. 2a,b** asterisk). Interestingly, a subset of GFP-labeled dermal sheath cup located at the base of the hair follicle expressed CD34 or PDGFRα (**Fig. 2b,c** arrow), and only a fraction of PDGFRα expressing dermal papilla cells were GFP-positive (**Fig. 2c** asterisk). Quantification of the GFP+/PDGFRα+ ratio revealed that telocytes constitute 50% and 40% of the dermal sheath and dermal papilla compartments, respectively (**Fig. 2d**). Cross-sections at the upper region of the hair follicle revealed that GFP+ telocytes in contact with the inner root sheath and hair shaft had low PDGFRα expression (**Fig. 2e**). Taken together, Foxl1/GFP telocytes represent a heterogenous population of cells.

In the intestine, telocytes compartmentalize mRNA molecules encoding important signaling proteins according to their position along the crypt-villus axis for localized signaling[36,44]. Therefore, we next examined the expression pattern of signaling molecules within telocytes along the hair follicle layers by smFISH to detect mRNAs encoding stem cell niche supporting factors focusing on Wnt-signaling. We stained skins from p30-33 Foxl1Cre; Rosa-mTmG mice at anagen. As shown in Figure 3A,3C, telocytes expressed both Wnt2b, which acts via canonical Wnt/β-catenin signaling, and Wnt5a, a member of the non-canonical branch of the pathway. However, the localization of the two mRNAs along the hair follicle layers was clearly distinct, with Wnt2b enriched at the dermal sheath cup and dermal papilla in close proximity to where lower bulb Lgr5 expressing cells reside (**Fig. 3a,b**) while Wnt5a mRNA molecules were detected in telocytes wrapping around the outer root sheath (**Fig. 3c**). Activation of canonical Wnt signaling in the hair germ progenitors at the onset of anagen has been shown to occur simultaneously with inhibition of BMP-

signaling[45-46]. Therefore, we examined the expression pattern of the mRNA molecules coding for the BMP inhibitor, Gremlin1 (Grem1). Similar to the expression pattern of Wnt2b, Grem1 mRNA molecules were detected at the dermal sheath, dermal sheath cup and dermal papilla in close proximity to the lower bulb, though with a broader expression domain (**Fig. 3d**), whereas Rspondin3 (Rspo3), an important Wnt agonist playing a role in hair follicle anagen duration[47], was detected in telocytes located at the luminal bulge region (**Fig. 3e**) and the dermal papilla (**Fig. 3f**). These results indicate spatial heterogeneity in the telocyte transcriptome in support of localized proliferation.

Unlike the intestine in which the epithelium is constantly self-renewed, hair growth is induced in cycles, in which stem cells of the bulge and hair germ regions are targeted to exit quiescence and enter active proliferation. To investigate the distribution of telocytes at the resting telogen phase in which stem cells in the bulge are in a quiescent state, we analyzed p21 Foxl1Cre; Rosa-mTmG mice. Whole mount and section analysis of skins co-stained with P-Cad, K15, or K14 demonstrated that telocytes expressing Foxl1, detected by smFISH (**Fig. 4e**), were distributed throughout the inter-follicular stroma (**Fig. 4a**). At this stage Foxl1-positive cells exhibit a condensed cellular structure with multiple short cytoplasmic processes (**Fig. 4a**), and were located at the dermal papilla (**Fig. 4b** asterisk) and along the hair follicle and interfollicular epidermis, in close contact with K15+ stem cells along the outer and encircled the inner bulge (**Fig. 4b,c**, **Videos 2a,b**). Close association of telocytes was also seen with αSMA+ arrector pili muscles (**Fig. 4d**). Strikingly, while we detected transcripts of Lgr5 mRNA in the quiescent bulge and hair germ (**Fig. 4f,g** red), critical niche molecules expressed in telocytes at anagen such as the Wnt ligand Wnt2b and the Wnt agonist Rspo3 were dramatically reduced in telogen telocytes (**Fig. 4f',g'** grey).

Thus, Foxl1-positive telocytes compartmentalize mRNA molecules encoding critical signaling molecules in space and time, suggesting a function in hair follicle proliferation.

Ablation of dermal telocytes results in cessation of hair follicle growth

In order to address the question of whether telocytes are important to hair follicle stem cell activity, we employed Foxl1-Cre; Rosa-mTmG/ iDTR mice (hereafter

referred to as iDTR), in which expression of the simian diphtheria toxin receptor (DTR) is activated in Foxl1+ cells through Cre-mediated excision of a stop cassette that renders telocytes responsive to diphtheria-toxin. This model enables cell-specific ablation of telocytes following toxin administration. Since Foxl1 is expressed in intestinal telocytes which are essential for intestinal homeostasis[35,36], in order to examine telocytes in the skin while maintaining their function in the intestine, we modified our diphtheria-toxin protocol to induce only partial ablation of telocytes (for details see methods). We induced cell ablation at the onset of anagen by injecting diphtheria toxin on p20-21, shaved back hair on p25, and sacrificed mice on p30-33 (**Fig. 5a,b**). iDTR mice exhibited modest growth retardation at the end of the experiment; however, this was not statistically significant (**Extended Data Fig. 2**). Strikingly, while on p30-33 hair bristles were clearly visible on the skin of control animals, iDTR mice showed naked and hairless pink skin (**Fig. 5c** asterisks indicating iDTR mice). As designed, diphtheria toxin induction resulted in a cell-specific ablation of GFP+ telocytes in iDTR mice compared with their control littermates (**Fig. 5d,e**). Sectioning and H&E staining revealed a complete cessation in hair follicle growth in the telocyte-deficient animals. Hair follicles of the iDTR mice on p30-33 remained arrested at telogen, whereas in control mice fully layered hair follicles extended down into the dermis and contained new hair shafts (**Fig. 5f,g**). Skin thickness in the iDTR was reduced by half compared to control littermates (**Fig. 5h**). Next, we determined epithelial proliferation by labelling cells in S-phase with a short pulse of the thymidine analogue EdU and analyzed stem cell distribution by staining for K15. As shown in figure 4I-K, stem and progenitor cell proliferation in iDTR was dramatically reduced compared to that of control mice. In control mice, the bulge K15-expressing stem cells (**Fig. 5i** green) were present at the upper part of the hair follicle, close to the epidermal compartment as is typical for anagen-phase hair follicles. In contrast, in the iDTR mice, remaining K15+ stem cells (**Fig. 5j** green) were distributed at the bottom of the permanent hair follicle, while only a few proliferating cells were observed at the hair germ, a typical feature of hair follicle at the onset of anagen. Therefore, telocytes are essential for hair follicle regeneration.

Ablation of dermal telocytes results in impaired Wnt-signaling

Hair follicle stem and progenitor cell proliferation is Wnt-dependent[7,8,10,13-15]; therefore, we hypothesized that the hair follicle growth cessation observed in the

iDTR mice is a result of inactive Wnt signaling. We found that nuclear localization of β-catenin, indicative of active Wnt signaling, was dramatically reduced in the hair follicles of iDTR mice following diphtheria toxin injections compared to controls, indicating a loss of canonical Wnt signaling (**Fig. 6a-c**). Next, we checked for the expression of the Wnt-target gene Sox9, which during the anagen phase is expressed in hair follicle stem cells at the bulge and by outer root sheath keratinocytes as shown in control mice (**Fig. 6d**). Following diphtheria toxin treatment, the number of Sox9-expressing cells in the bulge and outer root sheath was dramatically reduced in iDTR compared to control hair follicles, further supporting impaired Wnt signaling activity (**Fig. 6d-f**). These results indicate a role for telocytes in operating the Wnt-signaling pathway in the hair follicle at anagen phase.

Telocytes are a critical source of Wnt proteins essential for hair follicle regeneration

Since we found that telocytes are crucial for hair follicle regeneration, we wanted to directly test whether telocytes are a source of Wnt proteins important for hair follicle stem cell function. We used inducible Foxl1CreERT2 mice[43] crossed with mice carrying a floxed allele of the X-linked Porcn gene[48] to obtain Foxl1CreERT2; Porcn$^{loxP/Y}$ mice (hereafter referred to as Porcn∆). This model allows conditional elimination of all Wnt protein secretion from telocytes. Mice received three moderate tamoxifen doses, to mitigate intestinal injury, on p20-21 to p22-23 and the skin was analyzed on p30-33 (See **Fig. 7a** for experimental design). Porcn∆ mice showed a slight reduction in weight-gain starting on day 3 of tamoxifen induction when compared to control animals; however, this was not statistically significant (**Fig. 7b**). We sectioned the skin and found a reduction in skin thickness in Porcn∆ mice compared to control littermates and a complete cessation in hair follicle growth (**Fig. 7c-e**). While follicles in control mice showed typical anagen phase morphology, follicles of Porcn∆ mice did not enter into anagen and remained at the telogen phase of the hair cycle. We performed additional analysis of skin sections by EdU-labeling in combination with P-Cad and K15 staining (**Fig. 7f,g**) to follow proliferating hair germ/matrix cells and stem cells, or with Sox9 to label outer root sheath and stem cells or K14 to label keratinocytes (**Fig. 7i-j**). This analysis revealed typical quiescent

non-proliferating telogen phase hair follicle in Porcn∆ mice, in contrast to the proliferating anagen phase follicles in control mice (**Fig. 7f-k**). Next, we analyzed Wnt signaling activity by immuno-histochemistry for β-catenin. While β-catenin was localized to the nuclei of matrix cells in control hair follicles, β-catenin staining in Porcn∆ mouse hair follicles was only membranous (**Fig. 7l-n**). Thus, telocytes are a critical source of Wnt proteins necessary for hair follicle regeneration that cannot be compensated for by other, Foxl1-negative niche cells.

DISCUSSION

The skin and intestine are highly regenerative tissues, relying on niche signals to support stem cell function and replace short-lived differentiated cells. Here, we have identified a continuous inter- and sub-follicular network of Foxl1-expressing telocytes which form intimate contact with stem cells both in the quiescent and active states.

The telocyte network is heterogenous, composed in part of a fraction of mesenchymal components known to play an important role in hair follicle regeneration, such as the dermal sheath and dermal papilla. At telogen, telocytes are distributed throughout the skin stroma and located in close contact with stem cells, wrapping around the outer and inner regions of the hair bulge. This is interesting, as a mesenchymal component had not been reported previously within the luminal area of the bulge, to ours knowledge. Inter-follicular telocytes showed small and condensed cellular structures with multiple short cytoplasmic processes, whereas the ones in contact with the hair follicle were stretched and flat. Following anagen onset, however, telocytes' morphology changes, with a broad distended structure encapsulating the entire hair follicle along the outer root sheath, the deep inner root sheath and the hair shaft epithelial layers, and even intercalating among stem cells. Telocytes spatially compartmentalize mRNA molecules encoding niche-supporting factors to locally promote proliferation in a phase-dependent manner. Telocytes are crucial support for hair follicle regeneration by providing Wnt proteins essential for stem and progenitor cell proliferation; as shown by both ablation of dermal telocytes or removal of Wnt proteins from this niche compartment.

It has been suggested that a subset of dermal sheath cells which are retained following each hair cycle exhibit self-renewal properties and are a cellular source for repopulating the dermal sheath and the dermal papilla following anagen phase[49]. Although the telocyte network that is in close contact with the hair follicle is substantially extended during anagen compared to telogen, we have not detected telocyte proliferation in any of the phases. Further studies characterizing the dynamics in the expression profile, cellular morphology and distribution of telocytes during telogen-to-anagen transition will shed the light on the cellular and molecular mechanisms governing telocyte dynamics.

Together our findings reveal that telocyte function is not restricted to the intestine, and that these cells are an important source of Wnt proteins, essential for

stem cell function in the hair follicle. This demonstrates a general mechanism for maintaining homeostasis across epithelial tissues. Networks of telocytes in additional organs may not have been discovered due to the difficulty of observing thin, membranous cellular extensions sensitive to fixation. Unravelling the role of telocytes in stem cell function provides an important missing link between individual cell fate decisions to the maintenance of tissue homeostasis. The discovery of one cell type, telocytes, that contacts and potentially senses and signals all epithelial layers in at least two organ systems is a paradigm shift in our understanding of the mechanisms by which epithelial cell fate decisions are taken and morphogenetic fields are established.

ACKNOWLEDGMENTS

We thank all members of M. Shoshkes laboratory for helpful discussion. We thank C. Kalcheim and K.H. Kaestner for critical reading of the manuscript. E. Fuchs for her comments and feedback during the course of this study. S. Itzkovitz laboratory for assisting with implementing the smFISH technology. K.H. Kaestner for sharing mouse models. This work was supported by a research grant from the Israel Science Foundation (grant #1997/19, M.S.-C)

AUTHOR CONTRIBUTIONS

M.C wrote the manuscript, conceived, carried out experiments, analyzed and interpreted the data. S.N carried out mouse experiments and performed immunostaining. N.C and A.G performed smFISH experiments, I.B-P and M.S.-C designed and supervised the study. M.S.-C wrote the manuscript and directed the study.

DECLARATION OF INTERESTS

The authors declare no competing interests.

FIGURE LEGENDS

Figure 1. Foxl1 labels a network of mesenchymal cells with long cellular extensions which integrates with hair follicle epithelial layers.

(**a**) A diagram illustrating how the expression of membrane-bound GFP in Foxl1-cre-positive cells is driven in the Foxl1-Cre;Rosa-mTmG mouse model. (**b**) Spinning disk image of adult mouse whole back skin following tissue clearing and immunofluorescence staining for GFP (green) and EpCAM (grey) showing that GFP expression is restricted to subepithelial cells with small cell body and very long cellular extensions reaching hundreds of micron in length forming a network in contact with multiple hair follicles. Scale bar: 100µm. (**c-d**) At anagen Foxl1/GFP labeled cells form a comprehensive subepithelial sheath encapsulating the entire hair follicle. Confocal image of p30 mouse whole skin following tissue clearing and immunofluorescence staining for GFP (green) and P-cadherin (P-Cad grey). Scale bar: 100µm. (**e**) Representative smFISH image of p30 skin section hybridized for Foxl1 (smFISH grey) and immunofluorescence staining for GFP (green) showing the expression of Foxl1 mRNA transcripts along GFP labelled cells. (**e'**) zoom in on indicated region in E. Scale bar: 10µm. (**f-g**) Cross and longitudinal sections of hair follicles at the bulb region showing the distribution of Foxl1/GFP cells along the outer and inner epithelial layers, at the dermal sheath (F arrowhead), dermal sheath cup cell in contact with the bottom of the hair follicle (G arrow) and at the dermal papilla (**f-g** asterisk). GFP (green). Scale bar: 25µm. (H) Cross section of p30 hair follicle at the upper hair shaft region showing the distribution of Foxl1/GFP cells (green) along keratinocytes expressing K14 (red). Note the comprehensive network of Foxl1/GFP cells in close contact to epithelial cells. Scale bar: 25µm. (**i**) A 3D image of a cross section of p30 hair follicle at the bulge region showing Foxl1/GFP cells (green) in contact with K15 (red) stem cells. (**i'**) A slice view of (**i**) showing single optical sections of Foxl1/GFP cell stem cell contact. Scale bar: 3D 10µm, sections 5µm. (**j**) A diagram illustrating how induction with tamoxifen drives the expression of GFP in Foxl1-cre-positive cell bodies in the Foxl1 CreERT2; Rosa-mTmG mouse model. Mice were induced on p21 and analyzed on p30-33. (**k – l**) A z-series of confocal imaged optical sections showing the cell body of a single Foxl1/GFP cell (green)

intercalated among K15+ (red) stem cells at the bulge region at anagen phase. Experiments were repeated at least in three mice with similar results. Scale bar: 10μm.

Figure 2. Foxl1+ telocyte network consists a fraction of the dermal sheath and the dermal papilla components. (**a-c**) Sections of p30 Foxl1-Cre; Rosa-mTmG mouse skin co-stained for GFP (green) and αSMA (**a**), CD34 (**b**) or PDGFRα (**c, f**) in red, showing that telocytes represent a fraction of αSMA, PDGFRα, CD34 expressing dermal sheath (**a-c** arrowhead) and PDGFRα high dermal papilla (**a-c** asterisk). (**d**) Quantification of GFP+/PDGFRα+ ratio per hair follicle in percentages in the dermal sheath (mean= 52% ± 27) and the dermal papilla (mean=40% ± 22) (n=3 mice, 150 follicles for each chart). (**e**) Cross section at the upper hair shaft region showing GFP+ PDGFRα low expressing cells in contact with inner epithelial cell layers. Scale bar: 25μm.

Figure 3. Foxl1+ telocytes compartmentalize mRNA molecules of signaling proteins for localized signaling. (**a-f**) Representative smFISH images of p30 mouse skin stained for GFP (green) and hybridized as indicated. Note the expression of known stem cell niche supporting signals mRNA molecules (grey dots) Wnt2b (**a**), Gremlin1 (**d**) and Rspondin 3 (**e-f**), along telocytes in close proximity to the hair bulb expressing Lgr5 (**b**) and within the luminal area of the bulge (**e**), while non-canonical Wnt5a transcripts were detected along telocytes in contact with the outer root sheath (**c**). Experiments were repeated at least in three mice with similar results. Scale bar: 10μm.

Figure 4. At telogen, telocytes are present throughout the inter-follicular stroma, wrapping around the inner and outer bulge but express limited mRNA molecules encoding Wnt and Wnt inducer proteins. (**a-d**) Whole mount (**a**) and sections (**b-d**) of Foxl1-Cre; Rosa-mTmG p20-21 mouse skin co-stained for GFP (green) together with EdU incorporation and P-Cad (**a**), K15 (**b**), K14 (**c**) or αSMA (**d**) in red, showing the structure and distribution of telocytes at hair follicle telogen, throughout the interfollicular stroma, in contact with the hair germ P-Cad+ (**a**), at the dermal papilla (**b** asterisk), attached to the outer bulge K15+ (**b**), inner bulge K14+

(**c**) and arrector pili muscle αSMA+ (**d**). Note the structure of telocytes, small condensed with multiple short cellular processes along the inter-follicular stroma, stretched and elongated in contact with arrector pili muscles. Scale bar: 100μm. (**e-g**) Representative smFISH images of p20-21 mouse skin stained for GFP (green) and hybridized as indicated, showing the expression of Foxl1 along GFP+ telocytes in close contact with the bulge and hair germ expressing Lgr5 mRNA molecules (**f,g** red dots), but showing limited expression of the canonical Wnt2b and the Wnt inducer Rspo3 mRNA molecules (**f'-g'** grey dots). (**f', g'**) zoom in on indicated regions in f and g, respectively. Experiments were repeated at least in three mice with similar results. Scale bar: 10μm.

Figure 5. Ablation of dermal telocytes results in cessation of hair follicle growth. (**a**) A diagram illustrating induction of dermal telocyte ablation at the onset of anagen following diphtheria toxin induction in the Foxl1Cre; Rosa-mTmG/iDTR mouse model. (**b**) A scheme indicating experimental design: p21 mice at telogen phase, were injected with diphtheria toxin for four consecutive days, shaved four days following treatment on p25 and hair growth was monitored on p30-33. (**c**) A representative photograph of a litter of diphtheria-toxin treated mice. Note the pink back skin of iDTR mice (asterisks) compared to grey in control mice. (**d,e**) Confocal images of Foxl1Cre; Rosa-mTmG (Control) and Foxl1Cre; Rosa-mTmG/iDTR (iDTR) mice following diphtheria toxin treatment analyzed on p31 mouse skin sections stained for GFP (green) showing efficient ablation of dermal GFP^+ telocytes upon diphtheria toxin treatment. (**f,g**) H&E staining of control compared to iDTR skin sections of p30-33 mice. (**f', g'**) zoom in on indicated regions in F and G, respectively. Note the cessation in hair follicle growth and dramatic reduction in skin thickness in iDTR compare to control mice. (H) Quantification of skin thickness (n=3 mice per group <20 follicles for each bar ****P<0.0001, unpaired two-tailed t-test). (**i,j**) EdU incorporation (white), in control compared to iDTR mice (P-Cad, red; K15, green). Note the location of EdU+ proliferating cells in compare with K15+ stem cells, in controls at the hair bulb far deep from the bulge region, as is typical to anagen phase compared to iDTR mice in which few proliferating cells were detected close to the bulge region, as is typical to the onset of anagen phase. (**i', j'**) zoom in on indicated regions in i and j, respectively. (**k**) Quantification of EdU+ proliferating cells

per hair follicle. (n=3 mice per group <20 follicles for each bar ****P<0.0001, unpaired two-tailed t-test). Centre lines-mean, error bars- SD Scale bar: 100µm; zoom in 25µm.

Figure 6. Ablation of dermal telocytes results in impaired Wnt-signaling. (**a,b**) Immunohistochemistry for β-Catenin to analyze Wnt activity within the hair follicle. Nuclear β-Catenin staining, indicative of active Wnt-signaling, was dramatically reduced in iDTR (**b**) compared to control (**a**) mice. (**a',b'**) zoom in on indicated regions in a and b, respectively. (**c**) Quantification of nuclear β-Catenin+ cells per hair follicle (n=3 mice per group <20 follicles for each bar ****P<0.0001, unpaired two-tailed t-test). (**d,e**) Immunofluorescence staining for the Wnt target Sox9 (red), keratinocytes K14 (green) combined with EdU labelling (white). (**d',e'**) zoom in on indicated regions in d and e, respectively (**f**) Quantification of Sox9+ cells per hair follicle (n=3 mice per group <20 follicles for each bar ****P<0.0001, unpaired two-tailed t-test). Note the reduction in Sox9+ cells in iDTR compared to control hair follicles, further supporting impaired Wnt-signaling. Centre lines- mean; error bars- SD. Scale bar : 100µm; zoom in 25 µm.

Figure 7. Telocytes are a critical source of Wnt proteins essential for hair follicle regeneration. (**a**) A diagram illustrating induction of ablation of Wnt production from dermal telocytes at the onset of anagen following tamoxifen treatment in the Foxl1CreERT2; PorcnΔ mouse model and experimental design: at telogen, p21 mice were injected with tamoxifen for three consecutive days, shaved four days following treatment on p25 and hair growth was monitored on p30-33. (**b**) $Porcn^{\Delta/y}$ (Control, n=7) and Foxl1CreERT2; $Porcn^{\Delta/y}$ (PorcnΔ, n=10) mice were treated with tamoxifen and weighed every day. Weight was not statistically different in PorcnΔ compared to control mice (repeated measurements two-way ANOVA). (**c,d**) H&E staining of control compared to PorcnΔ skin sections of p30-33 mice. (**c',d'**) zoom in on indicated regions in c and d, respectively. Note the cessation of hair follicle growth in the PorcnΔ compared to control mice. (**e**) Quantification of skin thickness (n=3 mice per group <20 follicles for each bar ****P<0.0001, unpaired two-tailed t-test). (**f,g**) EdU incorporation (white) in cells at the bottom of the hair follicle, at the hair bulb, in control compared to the limited incorporation to the hair germ in

Porcn∆ mice (P-Cad, red; K15, green). (**f', g'**) zoom in on indicated regions in F and G, respectively. (**h**) Quantification of EdU+ proliferating cells per hair follicle (n=3 mice per group <20 follicles for each bar ****P<0.0001 unpaired two-tailed t-test). (**i,j**) Immunofluorescence staining for the Wnt target Sox9 (red), keratinocytes K14 (green) combined with EdU labelling (white). (**i', j'**) zoom in on indicated regions in I and J, respectively. (**k**) Quantification of Sox9+ cells per hair follicle (n=3 mice per group <20 follicles for each bar ****P<0.0001, unpaired two-tailed t-test). Note the reduction in Sox9+ cells in Porcn∆ compared to control hair follicles, supporting impaired Wnt-signaling (**l,m**) Immunohistochemistry for β-Catenin to analyze Wnt activity within the hair follicle. Reduced nuclear β-Catenin staining is observed in Porcn∆ (**m**) compared to control (**l**) mice further supporting impaired Wnt-signaling. (**l'-m'**) zoom in on indicated regions in l and m, respectively. (**o**) Quantification of nuclear β-Catenin+ cells per hair follicle (n=3 mice per group <20 follicles for each bar ****P<0.0001, unpaired two-tailed t-test). Centre lines- mean; error bars-SD. Scale bar: 100 μm; zoom in 25 μm.

METHODS

Foxl1-Cre; Rosa- mTmG/ iDTR, Foxl1-Cre; Rosa-mTmG, Foxl1-CreERT2; Rosa-mTmG, and Foxl1-CreERT2; Porcn∆ mice

Foxl1-Cre mice[50] were crossed with Rosa-inducible diphtheria toxin receptor (iDTR)[51] mice (Jackson Laboratories Bar Harbor, ME #007900) and or Rosa-membrane-targeted dimer tomato protein (mT) or membrane targeted green fluorescent protein (mG) (Rosa-mTmG)[52] (Jackson Laboratories Bar Harbor, ME #007900) to obtain Foxl1Cre; Rosa- mTmG/ iDTR or Foxl1Cre; Rosa-mTmG. Foxl1-CreERT2 mice[43] were crossed with Rosa-mTmG or Porcn-ex3-7Neo-flox[48] (Jackson Laboratories Bar Harbor, ME #020994) to obtain Foxl1CreERT2; Rosa-mTmG or Foxl1CreERT2; Porcn∆ mice. The Animal Care and Use Committee of the Hebrew University of Jerusalem approved all animal experiments.

Diphtheria toxin treatment

For Foxl1Cre; Rosa- mTmG/ iDTR and control, diphtheria toxin (Sigma-Aldrich #D0564) dissolved in 0.9% sodium chloride was administered intraperitonially at

20ng/g body weight. p20-21 mice were injected with diphtheria toxin for four consecutive days, once a day for the first two days and twice a day for the next two days at 8 h intervals.

Tamoxifen treatment

For Foxl1-creERT2; Porcn∆ or Foxl1-creERT2; Rosa-mTmG mice, tamoxifen (Sigma-Aldrich #10540-29-1) was dissolved in corn oil at a concentration of 30 mg/ml by shaking overnight at 37°C and administered intraperitoneally at 70 mg tamoxifen per kg body weight. p20 mice were injected on three consecutive days, sacrificed and analyzed on p30-33.

EdU incorporation and labelling

For EdU treatment 10 µM EdU solution was injected intraperitoneally, 1.5 h prior sacrificing mice. EdU was detected by 10µM Alexa Fluor™647 (Invitrogen # A10277), stained at RT for 30 min in a copper containing buffer (1mM CuSO4, 0.1M TRIS base, 10µM ascorbic acid).

Skin fixation with no perfusion

Mice were euthanized shaved and back skin was dissected. Skin was stretched on a Whatman paper and fixed in 4% PFA at 4°C overnight.

Fixation by trans-cardiac perfusion

Mice were anesthetized by intraperitoneal injection of 7.5% ketamine / 42.5% xylazine (v/v) and back skin was shaved. The thorax and ribcage were cut open to expose the heart. The right atrium was cut open and a 23G needle attached to a peristaltic pump was inserted into the left ventricle to pump pre-cooled (4°C) 4% PFA. Each mouse was perfused with ~30 mL fixative. skin was dissected and additionally fixed with 4% PFA at 4°C overnight.

Histology

For hematoxylin and eosin (H&E) staining, paraffin embedded tissue sections were rehydrated, incubated with hematoxylin (Sigma #0506002) for 5 min, rinsed with water, immersed in acid ethanol (70% EtOH/ 3% HCl (v/v)) for 10 s and washed with

water. Slides were immersed in 0.2% ammonium hydroxide (Sigma #338810), rinsed with water, immersed in eosin (Sigma #HT110116) for 40 s and briefly rinsed with tap water before dehydration and mounting.

Immunofluorescence and immunohistochemistry staining

Tissue was fixed by trans-cardiac perfusion. Antigen retrieval was performed using citrate buffer (pH=6) with a pressure cooker (Electron Microscopy Science). For immunofluorescence tissue was embedded in optimum cutting temperature compound (OCT) antibodies were diluted in CAS-Block (Invitrogen 008120). For β-catenin immunohistochemistry, tissue was embedded in paraffin, antigen retrieval was performed and antibodies were diluted in Starting block™ (Thermo Fisher #37542). Anti-mouse-biotin was used as a secondary antibody, VECTASTAIN ABC-HRP Kit, Peroxidase (Vector #PK-4000) was used to detect biotinylated molecules and 3,3-diaminobenzidine tetrahydrochloride (DAB) was used as a substrate to develop signal.

Clearing of mouse back skin X-CLARITY™

For clearing skin we employed Foxl1Cre;Rosa-mTmG p20-21, p30-33 or adult three month old mice. Tissue was fixed by trans-cardiac perfusion and skin was cleared for 6 h using an X-Clarity™ ETC chamber according to manufacturer's protocol (LOGOS Biosystems, Annandale, VA) as previously described[36].

Immunofluorescence staining of cleared whole tissue

Prior staining cleared skin was blocked with 10% fetal bovine serum in PBS for 1h. Primary and secondary antibodies were diluted in blocking solution containing 0.3% triton, incubated for 72 h at 4°C each. Finally, tissue was mounted *en bloc* on an image slide using 0.5mm thick adhesive silicon isolator mounted in Histodenz solution (88% Histodenz (w/v) in 0.02 M PBS).

Table 1. List of antibodies

Antibody	Catalogue #	Company	Dilution	Application
CD31	557355	BD Pharmingen	1:250	IF

CD34	14-0341-82	Thermo Fisher	1:100	IF
EpCAM	ab71916	Abcam	1:100	IF
GFP	AB-ab6673	Abcam	1:400	IF
GFP	NB100-1614	Novos Bio	1:400	IF
K14	906004	Biolegend	1:1000	IF
K15	833904	Biolegend	1:1000	IF
P- Cad	AF761-SP	R&D Systems	1:100	IF
PDGFRα	AF1062	R&D Systems	1:100	IF
SMA	ab5694	Abcam	1:250	IF
Sox9	AB-5535	Millipore	1:250	IF
β-Catenin	610153	BD Pharmingen	1:200	IHC
Anti-mouse biotin	705065147	Jackson Labs	1:100	IHC

Single molecule RNA FISH (smFISH)

Foxl1Cre;Rosa-mTmG p20-21 or p30-33 mice were employed. Tissue was fixed by trans-cardiac perfusion. Custom probe libraries were designed utilizing the Stellaris FISH probe designer software based on sequence to hybridize with a desired coding RNA (Biosearch Technologies, Inc., Petaluma, CA) and were coupled to Cy5. 7-micron cryo-sections were used for hybridization according to the protocol[53] with some adaptations. Briefly, tissue sections were digested with proteinase K (10 µg/ml Ambion AM2546) for 10 min and washed twice in 2× SSC (Ambion AM9765). Sections were washed in wash buffer (20% formamide, Ambion AM9342, 2× SSC) for 5 min and hybridized with smFISH probes diluted 1:3000 in hybridization buffer (10% dextran sulfate, Sigma D8906, 20% formamide, 1 mg/ml *E. coli* tRNA, Sigma R1753, 2× SSC, 0.02% BSA, Ambion AM2616, 2 mM vanadyl-ribonucleoside

complex, NEB S1402S) at 30°C overnight. Following hybridization, sections were washed with wash buffer containing 100 ng/ml DAPI at 30°C for 30 min. GFP antibody was diluted in hybridization buffer and Alexa 488 secondary antibody was diluted in GLOX buffer for 20 minutes, followed by DAPI (Sigma-Aldrich, D9542) staining.

Statistical analysis

All statistical and graphical data analyses were performed in GraphPad Prism 9.5.1. Number of replicates for each experiment and statistical tests are indicated in figure legends.

Microscopy

Microscopes used in the study:

Yokogawa w1 spinning disk attached to an inverted Nikon Ti2E microscope (Nikon, Japan).

Nikon Eclipse Ti2 Confocal System (Nikon, Japan).

Nikon TI2-LA-FL EPI-FL module for smFISH technology (Nikon, Japan).

Nikon DS-Fi2 color CCD camera attached to a Nikon Ti automated inverted microscope (Nikon, Japan).

Images were processed using Fiji, Imaris v10.0 or NIS Elements software packages.

SUPPLEMENTARY INFORMATION

Supplementary Figure 1. Visualization of telocyte network is impaired following standard tissue fixation protocols. (**a,b**) Representative confocal images of p31 Foxl1-Cre;Rosa-mTmG mouse whole back skin following standard fixation protocol and tissue clearing (for details see methods). EdU incorporation (white) and immunofluorescence staining for GFP (green), P-Cad (red) showing remnant of GFP signal along hair follicles at anagen in which much of the telocyte cellular structure is not visualized. Scale bar: 100µm.

Supplementary Figure 2. iDTR mouse growth is not statistically different from controls.
Rosa-mTmG/iDTR (Control, n=15 mice) and Foxl1Cre; Rosa-mTmG/iDTR mice (iDTR, n=5 mice) were treated with diphtheria toxin and weighed every day. Weight was not statistically different in iDTR and control mice. (repeated measurements two-way ANOVA).

Video 1. At anagen, telocytes along the inner bulge are in close contact with stem cells. A 20 µm cross section of Foxl1Cre; Rosa-mTmG p30 mouse skin at the hair follicle bulge region. Immunofluorescence staining for GFP (green), K15 (red) showing telocytes wrapping around the anagen inner bulge region in close contact to K15+ stem cells.

Video 2a. At telogen, telocytes are wrapping around the inner bulge. A 20 µm longitudinal section of Foxl1Cre; Rosa-mTmG p21 mouse skin. Immunofluorescence staining for GFP (green), K14 (red) showing the distribution of telocytes and their cellular processes at telogen along the inner bulge and at the dermal papilla.

Video 2b. At telogen, telocytes are distributed throughout the inter-follicular stroma, at the dermal papilla and in contact with the inner and outer bulge. A 20µm longitudinal section of Foxl1Cre; Rosa-mTmG p21 mouse skin. Immunofluorescence staining for GFP (green), K15 (red) showing the distribution of

telocytes at telogen, throughout the inter-follicular stroma, at the dermal papilla and outer and inner bulge region.

REFERENCES

1 Legue, E. & Nicolas, J. F. Hair follicle renewal: organization of stem cells in the matrix and the role of stereotyped lineages and behaviors. *Development* **132**, 4143-4154 (2005). https://doi.org:10.1242/dev.01975

2 Rompolas, P., Mesa, K. R. & Greco, V. Spatial organization within a niche as a determinant of stem-cell fate. *Nature* **502**, 513-518 (2013). https://doi.org:10.1038/nature12602

3 Xu, Z. *et al.* Embryonic attenuated Wnt/beta-catenin signaling defines niche location and long-term stem cell fate in hair follicle. *Elife* **4**, e10567 (2015). https://doi.org:10.7554/eLife.10567

4 Barker, N. *et al.* Identification of stem cells in small intestine and colon by marker gene Lgr5. *Nature* **449**, 1003-1007 (2007). https://doi.org:10.1038/nature06196

5 Sequeira, I. & Nicolas, J. F. Redefining the structure of the hair follicle by 3D clonal analysis. *Development* **139**, 3741-3751 (2012). https://doi.org:10.1242/dev.081091

6 Joost, S. *et al.* The Molecular Anatomy of Mouse Skin during Hair Growth and Rest. *Cell Stem Cell* **26**, 441-457 e447 (2020). https://doi.org:10.1016/j.stem.2020.01.012

7 Huelsken, J., Vogel, R., Erdmann, B., Cotsarelis, G. & Birchmeier, W. beta-Catenin controls hair follicle morphogenesis and stem cell differentiation in the skin. *Cell* **105**, 533-545 (2001). https://doi.org:10.1016/s0092-8674(01)00336-1

8 Gat, U., DasGupta, R., Degenstein, L. & Fuchs, E. De Novo hair follicle morphogenesis and hair tumors in mice expressing a truncated beta-catenin in skin. *Cell* **95**, 605-614 (1998). https://doi.org:10.1016/s0092-8674(00)81631-1

9 Maretto, S. *et al.* Mapping Wnt/beta-catenin signaling during mouse development and in colorectal tumors. *Proc Natl Acad Sci U S A* **100**, 3299-3304 (2003). https://doi.org:10.1073/pnas.0434590100

10 DasGupta, R. & Fuchs, E. Multiple roles for activated LEF/TCF transcription complexes during hair follicle development and differentiation. *Development* **126**, 4557-4568 (1999). https://doi.org:10.1242/dev.126.20.4557

11 Reddy, S. *et al.* Characterization of Wnt gene expression in developing and postnatal hair follicles and identification of Wnt5a as a target of Sonic hedgehog in hair follicle morphogenesis. *Mech Dev* **107**, 69-82 (2001). https://doi.org:10.1016/s0925-4773(01)00452-x

12 Reddy, S. T., Andl, T., Lu, M. M., Morrisey, E. E. & Millar, S. E. Expression of Frizzled genes in developing and postnatal hair follicles. *J Invest Dermatol* **123**, 275-282 (2004). https://doi.org:10.1111/j.0022-202X.2004.23215.x

13 Andl, T., Reddy, S. T., Gaddapara, T. & Millar, S. E. WNT signals are required for the initiation of hair follicle development. *Dev Cell* **2**, 643-653 (2002). https://doi.org:10.1016/s1534-5807(02)00167-3

14 Lowry, W. E. *et al.* Defining the impact of beta-catenin/Tcf transactivation on epithelial stem cells. *Genes Dev* **19**, 1596-1611 (2005). https://doi.org:10.1101/gad.1324905

15 Lo Celso, C., Prowse, D. M. & Watt, F. M. Transient activation of beta-catenin signalling in adult mouse epidermis is sufficient to induce new hair follicles but

continuous activation is required to maintain hair follicle tumours. *Development* **131**, 1787-1799 (2004). https://doi.org:10.1242/dev.01052

16 Beaudoin, G. M., 3rd, Sisk, J. M., Coulombe, P. A. & Thompson, C. C. Hairless triggers reactivation of hair growth by promoting Wnt signaling. *Proc Natl Acad Sci U S A* **102**, 14653-14658 (2005). https://doi.org:10.1073/pnas.0507609102

17 Ito, M. *et al.* Wnt-dependent de novo hair follicle regeneration in adult mouse skin after wounding. *Nature* **447**, 316-320 (2007). https://doi.org:10.1038/nature05766

18 Kwack, M. H., Kim, M. K., Kim, J. C. & Sung, Y. K. Dickkopf 1 promotes regression of hair follicles. *J Invest Dermatol* **132**, 1554-1560 (2012). https://doi.org:10.1038/jid.2012.24

19 Lim, X. *et al.* Interfollicular epidermal stem cells self-renew via autocrine Wnt signaling. *Science* **342**, 1226-1230 (2013). https://doi.org:10.1126/science.1239730

20 Lim, X., Tan, S. H., Yu, K. L., Lim, S. B. & Nusse, R. Axin2 marks quiescent hair follicle bulge stem cells that are maintained by autocrine Wnt/beta-catenin signaling. *Proc Natl Acad Sci U S A* **113**, E1498-1505 (2016). https://doi.org:10.1073/pnas.1601599113

21 Matos, I. *et al.* Progenitors oppositely polarize WNT activators and inhibitors to orchestrate tissue development. *Elife* **9** (2020). https://doi.org:10.7554/eLife.54304

22 Mok, K. W. *et al.* Dermal Condensate Niche Fate Specification Occurs Prior to Formation and Is Placode Progenitor Dependent. *Dev Cell* **48**, 32-48 e35 (2019). https://doi.org:10.1016/j.devcel.2018.11.034

23 Ouspenskaia, T., Matos, I., Mertz, A. F., Fiore, V. F. & Fuchs, E. WNT-SHH Antagonism Specifies and Expands Stem Cells prior to Niche Formation. *Cell* **164**, 156-169 (2016). https://doi.org:10.1016/j.cell.2015.11.058

24 Collins, C. A., Jensen, K. B., MacRae, E. J., Mansfield, W. & Watt, F. M. Polyclonal origin and hair induction ability of dermal papillae in neonatal and adult mouse back skin. *Dev Biol* **366**, 290-297 (2012). https://doi.org:10.1016/j.ydbio.2012.03.016

25 Rendl, M., Lewis, L. & Fuchs, E. Molecular dissection of mesenchymal-epithelial interactions in the hair follicle. *PLoS Biol* **3**, e331 (2005). https://doi.org:10.1371/journal.pbio.0030331

26 Hagner, A. *et al.* Transcriptional Profiling of the Adult Hair Follicle Mesenchyme Reveals R-spondin as a Novel Regulator of Dermal Progenitor Function. *iScience* **23**, 101019 (2020). https://doi.org:10.1016/j.isci.2020.101019

27 Reynolds, A. J. & Jahoda, C. A. Cultured dermal papilla cells induce follicle formation and hair growth by transdifferentiation of an adult epidermis. *Development* **115**, 587-593 (1992). https://doi.org:10.1242/dev.115.2.587

28 Grisanti, L. *et al.* Tbx18 targets dermal condensates for labeling, isolation, and gene ablation during embryonic hair follicle formation. *J Invest Dermatol* **133**, 344-353 (2013). https://doi.org:10.1038/jid.2012.329

29 Jahoda, C. A., Reynolds, A. J., Chaponnier, C., Forester, J. C. & Gabbiani, G. Smooth muscle alpha-actin is a marker for hair follicle dermis in vivo and in vitro. *J Cell Sci* **99 (Pt 3)**, 627-636 (1991). https://doi.org:10.1242/jcs.99.3.627

30 Heitman, N. *et al.* Dermal sheath contraction powers stem cell niche relocation during hair cycle regression. *Science* **367**, 161-166 (2020). https://doi.org:10.1126/science.aax9131
31 Martino, P. A., Heitman, N. & Rendl, M. The dermal sheath: An emerging component of the hair follicle stem cell niche. *Exp Dermatol* **30**, 512-521 (2021). https://doi.org:10.1111/exd.14204
32 Martino, P. *et al.* Progenitor-derived endothelin controls dermal sheath contraction for hair follicle regression. *Nat Cell Biol* **25**, 222-234 (2023). https://doi.org:10.1038/s41556-022-01065-w
33 Reynolds, A. J., Lawrence, C., Cserhalmi-Friedman, P. B., Christiano, A. M. & Jahoda, C. A. Trans-gender induction of hair follicles. *Nature* **402**, 33-34 (1999). https://doi.org:10.1038/46938
34 McElwee, K. J., Kissling, S., Wenzel, E., Huth, A. & Hoffmann, R. Cultured peribulbar dermal sheath cells can induce hair follicle development and contribute to the dermal sheath and dermal papilla. *J Invest Dermatol* **121**, 1267-1275 (2003). https://doi.org:10.1111/j.1523-1747.2003.12568.x
35 Aoki, R. *et al.* Foxl1-expressing mesenchymal cells constitute the intestinal stem cell niche. *Cell Mol Gastroenterol Hepatol* **2**, 175-188 (2016). https://doi.org:10.1016/j.jcmgh.2015.12.004
36 Shoshkes-Carmel, M. *et al.* Subepithelial telocytes are an important source of Wnts that supports intestinal crypts. *Nature* **557**, 242-246 (2018). https://doi.org:10.1038/s41586-018-0084-4
37 Ceafalan, L., Gherghiceanu, M., Popescu, L. M. & Simionescu, O. Telocytes in human skin--are they involved in skin regeneration? *J Cell Mol Med* **16**, 1405-1420 (2012). https://doi.org:10.1111/j.1582-4934.2012.01580.x
38 Chen, X. *et al.* Telocytes and their structural relationships with surrounding cell types in the skin of silky fowl by immunohistochemistrical, transmission electron microscopical and morphometric analysis. *Poult Sci* **100**, 101367 (2021). https://doi.org:10.1016/j.psj.2021.101367
39 Cretoiu, D. *et al.* FIB-SEM tomography of human skin telocytes and their extracellular vesicles. *J Cell Mol Med* **19**, 714-722 (2015). https://doi.org:10.1111/jcmm.12578
40 Romano, E. *et al.* A Two-Step Immunomagnetic Microbead-Based Method for the Isolation of Human Primary Skin Telocytes/CD34+ Stromal Cells. *Int J Mol Sci* **21** (2020). https://doi.org:10.3390/ijms21165877
41 Manole, C. G., Gherghiceanu, M., Ceafalan, L. C. & Hinescu, M. E. Dermal Telocytes: A Different Viewpoint of Skin Repairing and Regeneration. *Cells* **11** (2022). https://doi.org:10.3390/cells11233903
42 Sennett, R. *et al.* An Integrated Transcriptome Atlas of Embryonic Hair Follicle Progenitors, Their Niche, and the Developing Skin. *Dev Cell* **34**, 577-591 (2015). https://doi.org:10.1016/j.devcel.2015.06.023
43 Kolev, H. M. *et al.* A FoxL1-CreERT-2A-tdTomato Mouse Labels Subepithelial Telocytes. *Cell Mol Gastroenterol Hepatol* **12**, 1155-1158 e1154 (2021). https://doi.org:10.1016/j.jcmgh.2021.05.009
44 Bahar Halpern, K. *et al.* Lgr5+ telocytes are a signaling source at the intestinal villus tip. *Nat Commun* **11**, 1936 (2020). https://doi.org:10.1038/s41467-020-15714-x
45 Adam, R. C. *et al.* Temporal Layering of Signaling Effectors Drives Chromatin Remodeling during Hair Follicle Stem Cell Lineage Progression. *Cell Stem Cell* **22**, 398-413 e397 (2018). https://doi.org:10.1016/j.stem.2017.12.004

46 Kobielak, K., Stokes, N., de la Cruz, J., Polak, L. & Fuchs, E. Loss of a quiescent niche but not follicle stem cells in the absence of bone morphogenetic protein signaling. *Proc Natl Acad Sci U S A* **104**, 10063-10068 (2007). https://doi.org:10.1073/pnas.0703004104

47 Harshuk-Shabso, S., Dressler, H., Niehrs, C., Aamar, E. & Enshell-Seijffers, D. Fgf and Wnt signaling interaction in the mesenchymal niche regulates the murine hair cycle clock. *Nat Commun* **11**, 5114 (2020). https://doi.org:10.1038/s41467-020-18643-x

48 Liu, W. *et al.* Deletion of Porcn in mice leads to multiple developmental defects and models human focal dermal hypoplasia (Goltz syndrome). *PLoS One* **7**, e32331 (2012). https://doi.org:10.1371/journal.pone.0032331

49 Rahmani, W. *et al.* Hair follicle dermal stem cells regenerate the dermal sheath, repopulate the dermal papilla, and modulate hair type. *Dev Cell* **31**, 543-558 (2014). https://doi.org:10.1016/j.devcel.2014.10.022

50 Sackett, S. D., Fulmer, J. T., Friedman, J. R. & Kaestner, K. H. Foxl1-Cre BAC transgenic mice: a new tool for gene ablation in the gastrointestinal mesenchyme. *Genesis* **45**, 518-522 (2007). https://doi.org:10.1002/dvg.20315

51 Buch, T. *et al.* A Cre-inducible diphtheria toxin receptor mediates cell lineage ablation after toxin administration. *Nat Methods* **2**, 419-426 (2005). https://doi.org:10.1038/nmeth762

52 Muzumdar, M. D., Tasic, B., Miyamichi, K., Li, L. & Luo, L. A global double-fluorescent Cre reporter mouse. *Genesis* **45**, 593-605 (2007). https://doi.org:10.1002/dvg.20335

53 Farack, L. & Itzkovitz, S. Protocol for Single-Molecule Fluorescence In Situ Hybridization for Intact Pancreatic Tissue. *STAR Protoc* **1**, 100007 (2020). https://doi.org:10.1016/j.xpro.2019.100007

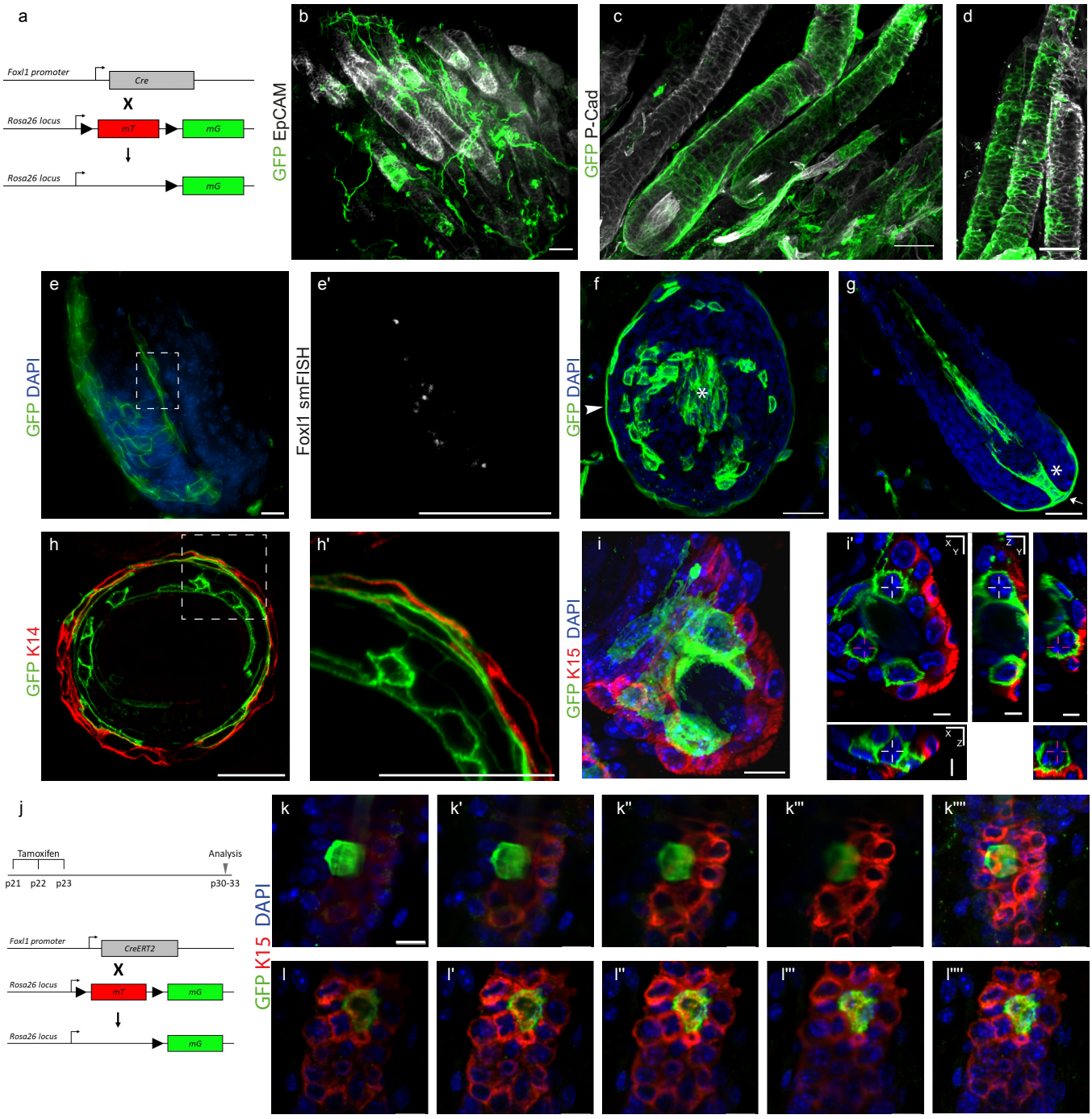
a
Foxl1 promoter
Cre
X
Rosa26 locus
mT
mG
Rosa26 locus
mG
b
GFP EpCAM
c
GFP P-Cad
d
e
GFP DAPI
e'
Foxl1 smFISH
f
GFP DAPI
g
h
GFP K14
h'
i
GFP K15 DAPI
i'
j
Tamoxifen
Analysis
p21 p22 p23
p30-33
Foxl1 promoter
CreERT2
X
Rosa26 locus
mT
mG
Rosa26 locus
mG
k
k'
k''
k'''
k''''
GFP K15 DAPI
l
l'
l''
l'''
l''''

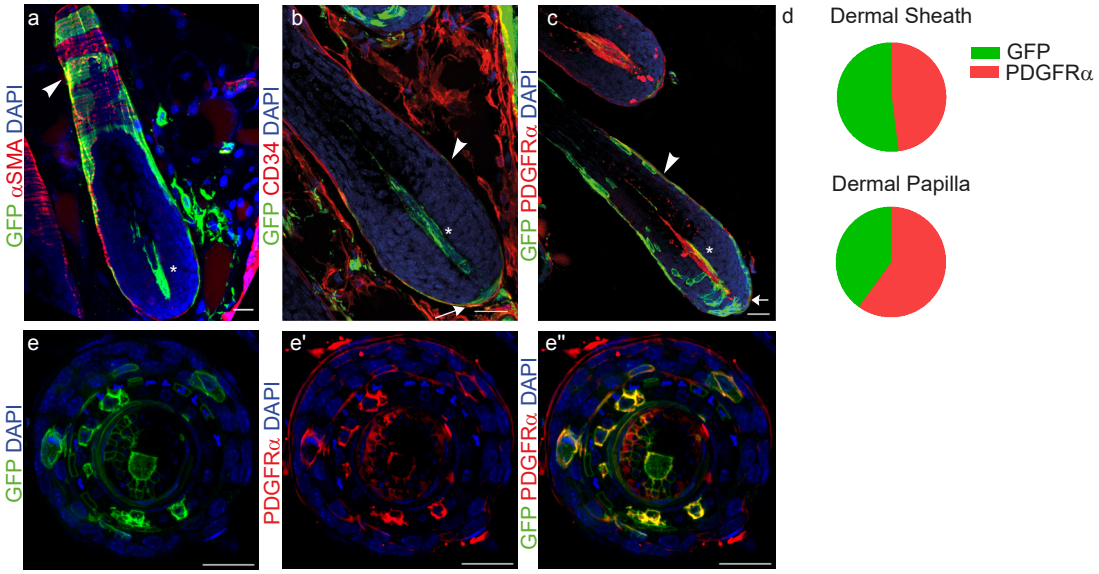
a
GFP αSMA DAPI
b
GFP CD34 DAPI
c
GFP PDGFRα DAPI
d
Dermal Sheath
GFP
PDGFRα
Dermal Papilla
e
GFP DAPI
e'
PDGFRα DAPI
e''
GFP PDGFRα DAPI

GFP Wnt2b smFISH DAPI
a
GFP Wnt2b smFISH
a'
Wnt2b smFISH
a''
GFP Lgr5 smFISH DAPI
b
GFP Lgr5 smFISH
b'
Lgr5 smFISH
b''
GFP Wnt5a smFISH DAPI
c
GFP Wnt5a smFISH
c'
Wnt5a smFISH
c''
GFP Grem1 smFISH DAPI
d
GFP Grem1 smFISH
d'
Grem1 smFISH
d''
GFP Rspo3 smFISH DAPI
e
GFP Rspo3 smFISH
e'
Rspo3 smFISH
e''
GFP Rspo3 smFISH DAPI
f
GFP Rspo3 smFISH
f'
Rspo3 smFISH
f''

a
GFP EdU P-Cad DAPI
b
GFP K15 DAPI
b'
c
GFP K14 DAPI
d
GFP αSMA DAPI
e
GFP DAPI
e'
GFP Foxl1 smFISH
f
GFP Lgr5 smFISH DAPI
f'
GFP Wnt2b smFISH
g
GFP Lgr5 smFISH DAPI
g'
GFP Rspo3 smFISH

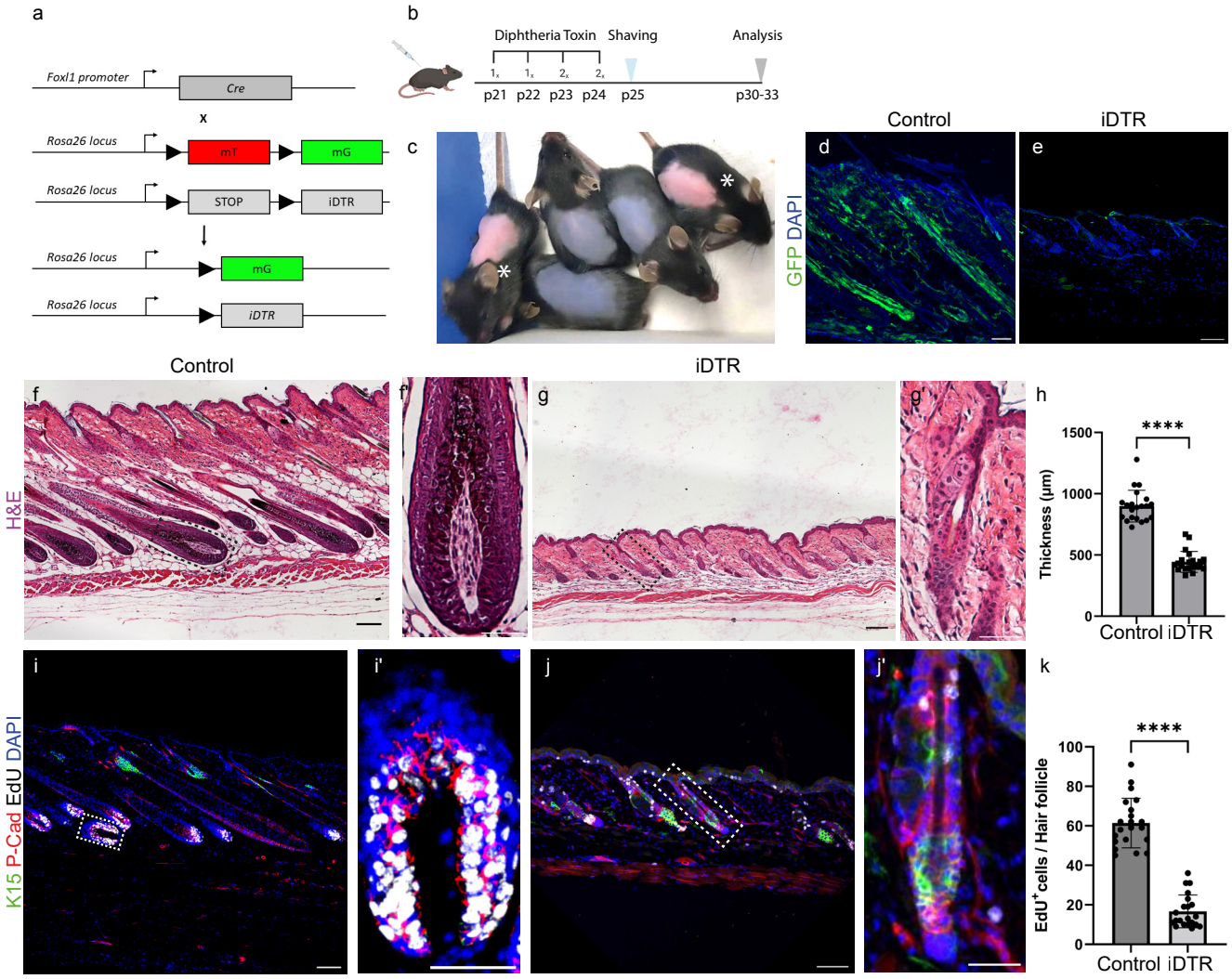
a
Foxl1 promoter
Cre
x
Rosa26 locus
mT
mG
Rosa26 locus
STOP
iDTR
Rosa26 locus
mG
Rosa26 locus
iDTR
b
Diphtheria Toxin
Shaving
Analysis
1x 1x 2x 2x
p21 p22 p23 p24 p25
p30-33
c
Control
iDTR
d
e
GFP DAPI
Control
iDTR
f
f'
g
g'
H&E
h
****
Thickness (µm)
1500
1000
500
0
Control iDTR
i
i'
j
j'
K15 P-Cad EdU DAPI
k
****
EdU+cells / Hair follicle
100
80
60
40
20
0
Control iDTR

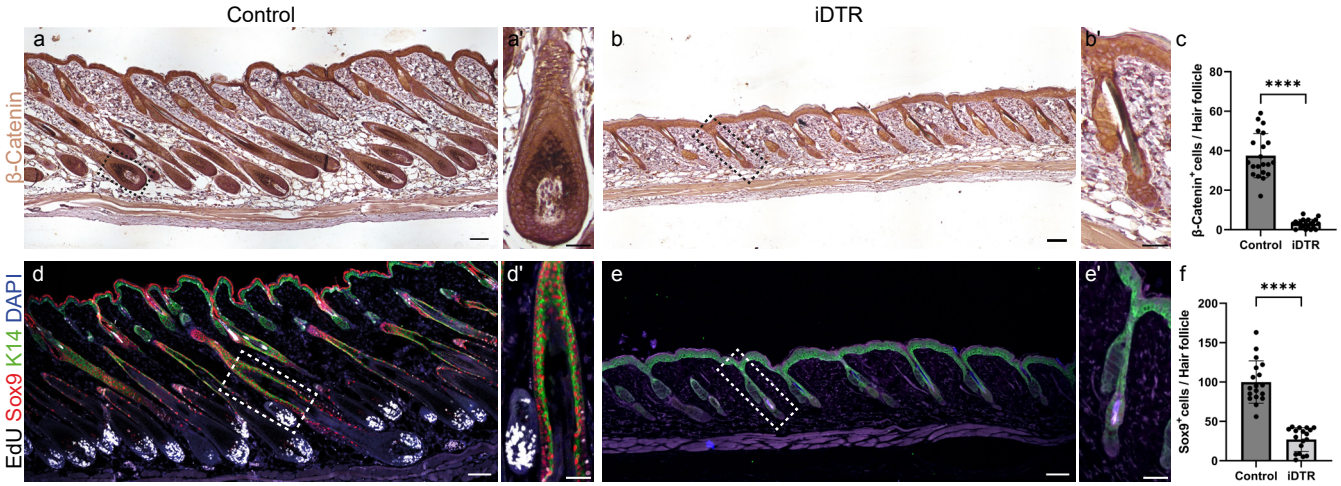
Control
iDTR
a
a'
b
b'
c
β-Catenin
β-Catenin+cells / Hair follicle
****
Control
iDTR
d
d'
e
e'
f
EdU Sox9 K14 DAPI
Sox9+cells / Hair follicle
****
Control
iDTR

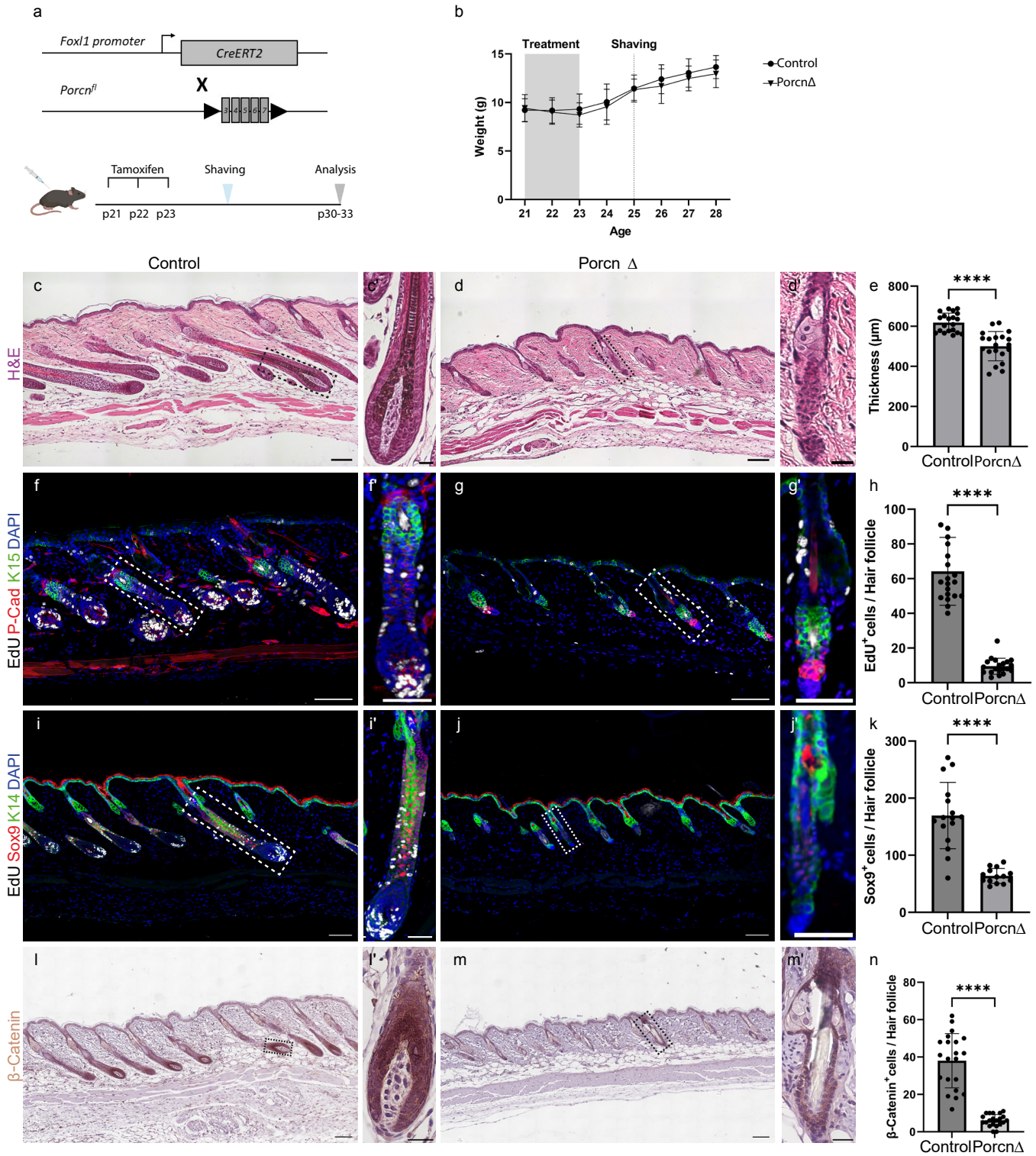
a
Foxl1 promoter
CreERT2
Porcn^fl
X
Tamoxifen
Shaving
Analysis
p21 p22 p23
p30-33
b
Treatment
Shaving
Weight (g)
Age
Control
PorcnΔ
Control
Porcn Δ
H&E
EdU P-Cad K15 DAPI
EdU Sox9 K14 DAPI
β-Catenin
Thickness (μm)
EdU+ cells / Hair follicle
Sox9+ cells / Hair follicle
β-Catenin+ cells / Hair follicle
****
Control
PorcnΔ